Title
Soil genesis and mineralogy across a volcanic lithosequence

Authors
Wilson, Stewart G
Lambert, Jean-Jacques
Nanzyo, Masami
et al.

Publication Date
2017

DOI
10.1016/j.geoderma.2016.09.013

Peer reviewed

Geoderma 285 (2017) 301–312

Contents lists available at ScienceDirect

Geoderma

journal homepage: www.elsevier.com/locate/geoderma

Soil genesis and mineralogy across a volcanic lithosequence

Stewart G. Wilson [a,*], Jean-Jacques Lambert [b], Masami Nanzyo [c], Randy A Dahlgren [a]

[a] Land, Air and Water Resources Department, University of California-Davis, 1 Shields Ave, 95616 Davis, CA, United States
[b] Department of Viticulture and Enology, University of California-Davis, 1 Shields Ave, 95616 Davis, CA, United States
[c] Graduate School of Agricultural Science, Tohoku University, 1-1 Tsutsumidori-Amamiyamachi, Aoba-ku, Sendai, Miyagi 981 8555, Japan

ARTICLE INFO

Article history:
Received 30 June 2016
Received in revised form 2 September 2016
Accepted 11 September 2016
Available online xxxx

Keywords:
Pedogenesis
Lithology
Lithosequence
Volcanic soils
Halloysite
Mineralogy

ABSTRACT

Lithology is a principle state factor of soil formation, interacting with climate, organisms, topography and time to define pedogenesis. A lithosequence of extrusive igneous lithologies (rhyolite obsidian, dacite, andesite and basalt) was identified in the Clear Lake Volcanic Field in the Coast Range of northern California to determine the effects of lithology on pedogenesis, clay mineralogy and soil physiochemical properties. Based on regional landscape erosion rates (0.2–0.5 mm yr^{-1}), the soil residence times for the investigated pedons (~150 cm deep) were of the order of 3000 to 7500 years indicating that the soils developed under the relatively stable Holocene mesic/xeric climate regime. Soils from all lithologies developed to a similar Xeralf taxonomy with remarkably consistent physiochemical properties. Although total (Fe_t) and dithionite-citrate extractable (Fe_d) iron concentrations diverged across lithologies, the degree of weathering as assessed by the Fe_d/Fe_t ratio was similar across the lithosequence. In spite of large differences in silica content of the parent materials, the clay mineralogical assemblage of all lithologies was dominated by kaolin minerals (kaolinite and/or halloysite). All pedons displayed an increase in halloysite and the degree of halloysite hydration with increasing depth, except the basalt pedon, which was dominated by kaolinite with only trace halloysite. We attribute this lack of halloysite in the basalt pedon to the lower silica activities associated with this silica-poor lithology. There was a lack of nanocrystalline minerals across all lithologies as inferred from selective dissolution. The dominance of crystalline materials is a function of the xeric soil moisture regime whereby summer soil profile desiccation promotes dehydration and crystallization of metastable nanocrystalline precursors. Further, the pronounced summer dry period results in dehydration of halloysite (1.0 nm) to halloysite (0.7 nm; also referred to as meta halloysite in some literature), together with transformation to kaolinite, in the upper soil profile. In spite of the relatively young soil residence times of these soils (Holocene age), the effects of lithology persisted only in differences in Fe oxide concentrations (Fe_d), as well as a lack of significant halloysite in basalt pedons. The overwhelming effect of climate in these highly weatherable parent materials narrowed the trajectory of pedogenesis, resulting in soils from contrasting lithologies converging on kaolin mineralogy, a lack of nanocrystalline constituents, and similar soil physiochemical properties.

1. Introduction

Lithology is a master variable of pedogenesis (Jenny, 1994). The interaction of lithology with other factors such as climate and biology is a chapter in the story of life on Earth (Lenton et al., 2012), influencing global climate (Chadwick et al., 1994), primary productivity (Morford et al., 2011), the distribution of plants (Hahm et al., 2014), and the genesis of soils (Jenny, 1994). Lithology is a dominant factor in the early stages of pedogenesis, and yet very few pure lithosequences have been investigated owing to the difficulty of constraining the other soil forming factors, particularly climate (Jenny, 1994). With time, and under the influence of climate, the effect of parent material on soil mineralogy and physiochemical properties is thought to diminish, although the time required for parent material effects to be subdued is uncertain (Chesworth, 1973). Here we present a novel, well-constrained volcanic lithosequence that spans the breadth of extrusive igneous (i.e. hard rock) lithologies (rhyolite, dacite, andesite and basalt) to investigate the influence of lithology on pedogenesis, soil physiochemical properties and clay mineralogy. Understanding the role of lithology in pedogenesis is important for soil survey, ecological/biogeochemical modeling, agronomy/soil fertility and land-use management.

Previous investigations of lithosequences have attributed differences in soil morphologic and physical attributes to lithology. Schaetzl (1991) noted the influence of coarse fragments and texture on pedogenesis and plant distribution. Parsons and Herriman (1975) concluded that differences in grain size between schist, granite and pyroclastic materials contributed to differences in soil physiochemical properties and

* Corresponding author.
E-mail address: stuwilson@ucdavis.edu (S.G. Wilson).

http://dx.doi.org/10.1016/j.geoderma.2016.09.013
0016-7061/

morphology. In Greece, soils in marble and dacite were finer textured, while soils in gneiss, granite and diorite were coarser textured (Yassoglou et al., 1969). Similarly, differences in soil texture and erodability were observed in soils in the Sierra Nevada of California formed in granodiorite, quartzite and basalt (Willen, 1965). These studies attributed many of the physical differences observed in soils to differences in the initial grain size of the parent materials; however, all these studies lacked investigations of clay mineralogy.

Within the few lithosequences that have included investigations of clay mineralogy, no clear trends of lithologic influence on clay mineralogy were identified. Hoyum and Hajek (1979) identified mixtures of smectitic and halloysitic clays in soils formed in coastal plain sediments, with halloysite in common to all soils, whereas Hutton (1951) concluded that the common weathering environment resulted in the dominance of smectitic clays in a loess climo-lithosequence. Anderson et al. (1975) observed predominantly smectitic clays in soils on limestone, and kaolinitic clays in soils on sandstone, likely due to differences in carbonates, pH, base cation content, and drainage. Levine et al. (1989) concluded that more permeable dolomitic limestone encouraged the formation of smectite through the dissolution of dolomite and release of Mg, while impervious limestone limited smectite formation. Mareschal et al. (2015) investigated soils formed in granites with differing grain sizes, and found differences in particle size, cation exchange capacity (CEC), and extractable Fe and Al, but not clay mineralogy. Similarly, Yousefifard et al. (2015), investigated a lithosequence including intrusive igneous rocks (granites and diorites) and extrusive igneous rocks (andesites and a dacite), and found differences in soil physicochemical properties, but no significant differences in clay mineralogy (smectite), which the authors attributed to the common arid/semiarid climate. Alternatively, Heckman and Rasmussen (2011) found vast differences in CEC, clay content and Fe-oxides, as well as clay mineralogy and mass flux, between rhyolite and basalt. Of these lithosequences, no consistent trends were evident for the influence of lithology on clay mineral formation. Furthermore, none of these lithosequences contained exclusive investigations of intrusive or extrusive igneous lithologies, and none spanned the range of silica compositions from felsic to mafic inclusively.

In contrast to previous findings on lithosequences that suggest divergence in clay mineralogy and soil physical and morphologic factors, climosequences in the mesic/xeric climate of California point to similarities in morphology and clay mineralogy in climatic zones of intense weathering, where the trajectory of pedogenesis appears to be narrowed due to the overwhelming influence of climate. Climosequences in basalt (Rasmussen et al., 2010), andesite (Takahashi et al., 1993; Rasmussen et al., 2007) and granite (Dahlgren et al., 1997a) identified zones of intense weathering at similar elevations and climates (mesic/xeric) where mild wet winters, and dry hot summers favor desilication, clay generation and illuviation, and crystalline phyllosilicate and Fe-oxide clay minerals.

To address these contrasting findings from lithosequences and climosequences, a well-constrained lithosequence of extrusive igneous materials that spans the range of felsic (rhyolite) to mafic (basalt) lithologies was identified in the Clear Lake Volcanic Field in the northern Coast Range of California. All lithologies were located in relatively close geographic proximity (within a 15 km radius) and the soils are believed to have primarily developed under Holocene climate conditions consisting of a mesic/xeric, temperature/moisture regime, with similar rates of denudation. Factors such as climate and soil residence time are relatively well constrained. By maintaining other pedogenic state factors constant, while varying the elemental composition of the parent material, this investigation seeks to identify the influence of lithologic composition on soil genesis, clay mineralogy, Fe-oxide generation, and soil physiochemical properties.

2. Materials and methods

2.1. Site description

The volcanic lithosequence is located within the Clear Lake Volcanic Field (CLVF), an active, late Pleistocene volcanic center in the northern California Coast Range, where regional deformation associated with the San Andreas Fault activates mafic to felsic eruptions (Fig. 1) (Hearn et al., 1975, 1995). The CLVF consists of a range of lithologies (rhyolite to basalt) in a complex of domes, flows and pyroclastic deposits (Hearn et al., 1975; Donnelly-Nolan et al., 1981). Four pedons were investigated from four lithologies of diverse chemical composition, but similar hard rock physical composition derived from flows in the CLVF, namely rhyolitic obsidian, dacite, andesite and basalt, all coexisting in the same climate and having a similar porphyritic character. The SiO_2 content of parent materials ranged from 55% in the basalt to 75% in the rhyolite (Hearn et al., 1995). Mean landscape erosion rates in the area are 0.2–0.5 mm yr^{-1} and uplift rates are ~0.3 mm yr^{-1}, corresponding to soil residence times for a 150-cm deep pedon of 3000 to 7500 years (Balco et al., 2013). These residence times constrain pedogenesis to relatively stable Holocene climate conditions. The climate is Mediterranean (xeric soil moisture regime, Soil Survey Staff, 2014a), with mild wet winters and warm dry summers. The mean annual soil temperatures are between 14 and 16 °C (mesic/thermic boundary, soil temperature regime, Soil Survey Staff, 2014a) and mean annual precipitation is ~640 mm, mostly occurring as rainfall in November to March. The dominant vegetation community at all sites was oak woodland (*Quercus – douglasii, kelloggii, wislizeni*) with minor pine (*Pinus - ponderosa, sabiniana*), and with annual grasses in the understory, with some recent conversion to winegrape production. Following fire, which has an average historical return frequency of 0–35 years for low severity fires, a chaparral shrub community dominated by *Quercus dumosa, Ceanothus* spp., *Arctostaphylos* spp., and *Adenostoma fasciculatum* is a common plant community. All sampling sites were on shoulder positions, with similar slope (15–20%) and aspect (southern).

2.2. Soil characterization

Soils were described in the field, sampled by genetic horizon, air-dried and sieved to isolate the <2-mm fraction. Soils were size fractionated using pipette and wet sieving methods (Soil Survey Staff, 2014b). Briefly, 10 g of air-dried soil were pretreated with 5% H_2O_2 for organic matter removal (Soil Survey Staff, 2014b), citrate-dithionite for Fe-oxide removal (Holmgren, 1967) and then dispersed with dilute sodium hexametaphosphate. Dispersed samples were wet sieved through a 53 μm screen, and the clay and silt (<53 μm fraction) collected for subsequent pipette analysis. Sands (>53 μm) were collected, dried at 105 °C, and weighed.

Soil pH was measured 1:2 soil:solution in H_2O, 0.01 M $CaCl_2$, and 1.0 M KCl (Soil Survey Staff, 2014b). Organic C and N were measured on ground samples (<125 μm) with an ECS 4010 CHNSO Analyzer (Costech Analytical Technologies, Inc., California, USA). Phosphate retention was determined using the method of Blakemore et al. (1981). CEC and extractable cations were measured with 1 M NH_4OAc (pH 7.0) extraction (Soil Survey Staff, 2014b). Base saturation was calculated from the sum of bases extracted by 1 M NH_4OAc. Pedon Fe_d, clay, and organic carbon pools (kg m^{-2}) for the upper 120 cm of each pedon were calculated based on field estimations of coarse fragment volume and bulk density estimates of 1.2 g cm^{-3} for A horizons, 1.3 g cm^{-3} for AB horizons and 1.5 g cm^{-3} for B horizons obtained from NRCS soil survey pedon description data.

2.3. Mineralogical analysis

X-ray diffraction (XRD) was performed on the clay-size fraction (<2 μm). XRD analyses were made with a Rigaku Ultima IV (Rigaku,

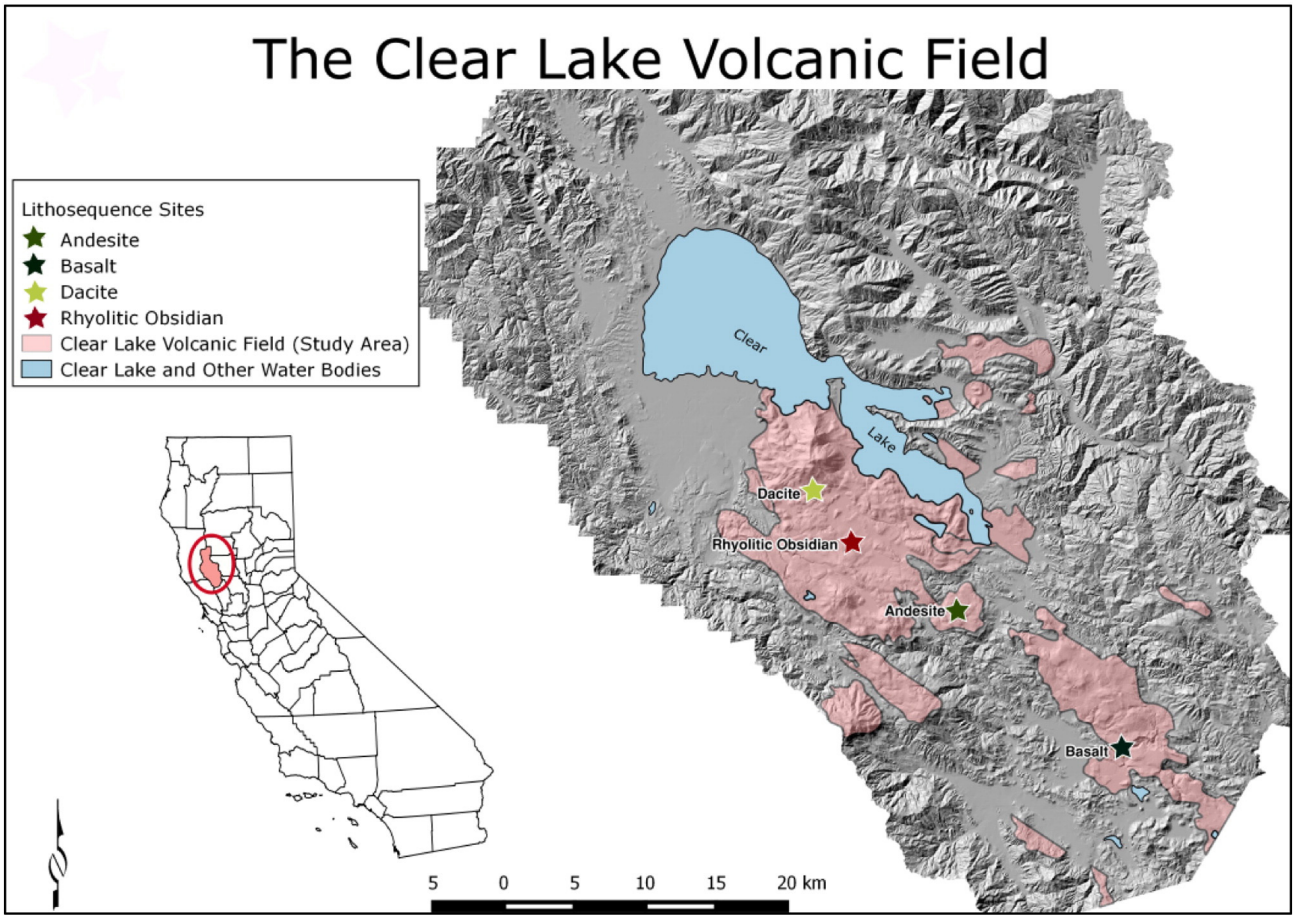

Fig. 1. The Clear Lake Volcanic Field study site. Inset map, California county boundaries.

Tokyo, Japan) producing Cu-Kα radiation generated with 40-kV accelerating potential and 40-mA tube current. Clays were oriented on glass slides, and subjected to standard treatments: Mg-saturation, Mg-saturation plus glycerol solvation, K-saturation (25 °C) and heat treatment of the K-saturated slides at 350 °C and 500 °C. Additionally, the Mg-saturated slides were treated with formamide to distinguish kaolinite from dehydrated halloysite based on a peak shift for dehydrated halloysite from 0.7 to 1.0 nm with formamide intercalation (Churchman et al., 1984).

Transmission electron microscopy (TEM) observations were performed using a Hitachi-7650 operating at 100 kV. For observation, citrate-dithionite-treated (deferrated) clay specimens were spotted onto carbon-coated collodion films. Scanning electron microscopy (SEM) of Pt-Pd coated, deferrated clay specimens was performed using a Hitachi SU8000 operated at 15 kV. EDX analysis was performed to examine the elemental composition of the clay specimens.

Nonsequential selective dissolution in acid ammonium-oxalate and citrate-dithionite was used to characterize Fe, Al and Si in pedogenic pools. For ammonium-oxalate extraction, samples were shaken with 0.2 M ammonium oxalate for 4 h in the dark with a soil:oxalate ratio of 1:100 to extract Al, Fe, and Si (Al_o, Fe_o, and Si_o) from organic complexes and nanocrystalline Fe-(hydr)oxides (e.g., ferrihydrite) and nanocrystalline and paracrystalline aluminosilicates (allophane and imogolite, respectively) (Soil Survey Staff, 2014b). Citrate-dithionite extraction (Fe_d, Al_d and Si_d) consisted of treating 2 g of soil with 2 g sodium dithionite, 20 g sodium citrate and 120 ml of water, with shaking for 14 h (Holmgren, 1967). All extracts were treated with "Superfloc" and centrifuged before analysis via ICP-OES for Fe, Al and Si.

2.4. Total elemental analysis

Total elemental analysis of the fine-earth fraction (<2 mm) was performed on duplicate 5 g samples of air-dried soils pulverized to a fine powder (<125 μm). Subsamples of the pulverized soil were placed in a XRF cup and the opening covered with Mylar film secured with a plastic collar. Samples were analyzed for Fe, Al, Si, Ca, Mn and Ti using a Thermo Scientific Xlt 600 XRF and the ex-situ analysis procedure. Prior and following sample analysis, calibration was performed/verified with soil standard NCS DC 73308 (Thermo #180-600).

3. Results

3.1. Soil characterization

Soil pH in H_2O was generally well constrained across the lithosequence (Table 1). However, pH in H_2O in the rhyolitic obsidian pedon declined a full unit from 6.8 to 5.5 from the Ap2 to the 2Bt1 horizon suggestive of, along with data presented later, a lithologic discontinuity. Soil pH in KCl, was similar across the lithosequence (5.2 ± s.e. 0.1), with six horizons below 5.0. Delta pH (pH KCl-pH H_2O) ranged from −0.7 to −1.6 across the lithosequence, indicating a dominance of permanent negative charge as opposed to variable charge constituents (Rasmussen et al., 2010; Soil Survey Staff, 2014b).

CEC was generally low (<19 $cmol_c\ kg^{-1}$) and base saturation high (>72%) among pedons. Base saturation of argillic horizons increased with increasingly mafic composition (i.e., from rhyolite to basalt) across the lithosequence, increasing from 71.5% in the rhyolite pedon to 88% in

Table 1
Physical, taxonomic and chemical characterization data for soils across volcanic lithosequence in northern California.

Lithology	Horizon	Depth (cm)	Munsell color		Sand	Silt	Clay	D_b[a]	pH			CEC-7[b]	BS[c]	N	C	C:N
			Dry	Moist	g kg^{-1}			g cm^{-3}	H_2O	$CaCl_2$	KCl	($cmol_c$ kg$_{-1}$)	%	g kg^{-1}		
Rhyolite																
Clayey-skeletal, halloysitic, mesic, ultic haploxeralf	Ap1	0–10	10YR 4/3	10YR 3/2	477	315	208	1.2	6.7	6.2	5.8	11	96	3.4	61.6	18.1
	Ap2	10–30	10YR 5/3	10YR 3/3	390	377	233	1.2	6.8	6.2	5.6	11.7	88	0.7	17.9	25.6
	2AB	30–55	10YR 6/3	7.5YR 4/3	357	372	271	1.35	6.0	6.1	5.3	9.6	81	0.2	4.1	20.5
	2Bt1	55–118	7.5YR 6/3	7.5YR 5/8	168	50	782	1.5	5.5	5.4	4.8	12.7	72	0.1	2.8	28.0
	2Bt2	118–155	7.5YR 6/3	7.5YR 5/6	156	81	763	1.5	5.4	5.1	4.5	13.3	72	0.1	2.3	23.0
Dacite																
Fine, halloysitic, mesic, typic palexeralf	A1	0–16	7.5YR 3/4	7.5YR 3/2	284	345	372	1.1	6.2	5.5	5.1	16.2	77	2.1	63.3	30.1
	A2	16–30	7.5YR 4/4	5YR 3/4	205	377	418	1.2	6.7	5.9	5.4	12.4	89	0.7	15	21.4
	ABt	30–49	7.5YR 5/6	5YR 3/4	184	364	452	1.35	6.6	5.8	5.2	12.1	83	0.3	6.9	23.0
	Bt1	49–74	7.5YR 5/6	5YR 4/4	139	381	481	1.5	6.4	5.6	5.0	12.3	83	0.2	3.9	19.5
	Bt2	74–97	10 YR 6/4	7.5YR 4/4	110	397	494	1.5	6.2	6.1	5.1	13.2	85	<0.01	2.3	NA
	Bt3	97–117	10 YR 6/4	7.5YR 4/4	100	421	480	1.5	6.3	5.8	5.0	13.6	88	ND	1.9	NA
	BCt	117–150	10YR 6/3	7.5YR 4/4	88	425	487	1.5	6.3	5.8	4.7	19	85	<0.01	2.1	NA
Andesite																
Fine, halloysitic, mesic, typic palexeralf	A1	0–28	10YR 3/4	10YR 3/2	321	352	326	1.2	6.2	5.5	5.0	9.3	79	1.6	29.2	18.3
	ABt	28–79	7.5YR 5/4	5YR 3/4	208	372	419	1.2	6.2	5.4	4.9	9.5	81	0.2	4.5	22.5
	Bt1	79–99	10YR 5/6	5YR 3/4	197	357	446	1.5	6.1	5.5	5.0	9.7	85	0.2	3.5	17.5
	Bt2	99–152	10YR 6/6	7.5YR 3/4	168	344	488	1.5	6.1	5.6	5.1	8.7	85	<0.01	1.7	NA
	BCt	152–191	10YR 5/4	7.5YR 3/4	224	348	429	1.5	5.9	5.5	4.9	9.6	85	ND	1.5	NA
Basalt																
Fine, kaolinitic, mesic, typic haploxeralf	A1	0–7	5YR 3/3	5YR 2.5/2	303	357	339	1.2	6.4	6.2	5.4	17.1	86	2.6	50.6	19.5
	A2	7–21	5YR 3/4	5YR 3/3	238	373	389	1.2	6.7	6.2	5.5	14.7	90	0.8	15.3	19.1
	Bt1	21–37	5YR 4/4	5YR 3/3	177	367	456	1.5	6.7	6.2	5.5	13.9	88	0.4	7.9	19.8
	Bt2	37–66	5YR 4/4	5YR 3/3	170	338	492	1.5	6.6	6.1	5.4	15.6	86	0.4	6.6	16.5
	Bt3	66–100	5YR 4/4	5YR 3/4	135	279	586	1.5	6.3	5.8	5.1	16.3	83	0.3	6	20.0
	BC	100–120	5YR 4/4	5YR 4/4	130	244	626	1.5	6.0	5.6	4.8	18.1	77	0.3	5.4	18.0

[a] Bulk density.
[b] Cation exchange capacity by ammonium acetate pH 7.
[c] Base saturation by sum of cations.

the basalt pedon. A "pumiceous carapace" or a thin deposit of pumice as described by Hearn et al. (1995), which overlays the rhyolitic obsidian flows in some localized areas, may have contributed to the enrichment of bases and the elevated pH in A horizons of the rhyolite pedon. CEC was similar among pedons (12.8 ± s.e. 0.61 $cmol_c$ kg^{-1}), ranging from 9.7 to 13.9 $cmol_c$ kg^{-1} in Bt horizons. The ratio of CEC to clay percent ranged from 0.18 to 0.53 (0.31 ± s.e. 0.02) indicating subactive to active cation exchange activity classes (Soil Survey Staff, 2014a). Soil color displayed increased reddening with increasingly mafic composition, trending from 10YR in the rhyolite pedon to 5YR in the basalt pedon.

Clay contents in argillic horizons ranged from 446 g kg^{-1} in the Bt1 horizon of the andesite soil to 782 g kg^{-1} in the 2Bt1 horizon of the rhyolitic obsidian pedon (average of all horizons = 454 ± s.e. 30 g kg^{-1}). Normalized for coarse fragments and bulk density and calculated as kg m^{-2} in the upper 120 cm of the pedon, clay production was similar across the lithosequence, with the basalt pedon having slightly higher clay production (Fig. 2a). Organic carbon contents were enriched in surface horizons of all pedons, and were notably lower (21–34 g kg^{-1} lower) in the andesite A1 horizon. However, when represented on a pedon basis, no consistent trend in carbon storage attributable to lithology was evident (Fig. 2c).

3.2. Selective dissolution, P-retention and total elemental analysis

Dithionite-extractable Fe (Fe_d) increased with increasing mafic composition of the parent material: rhyolite < dacite ≈ andesite < basalt (Table 2, Fig. 3a). The amount of Fe_d generated in the upper 120 cm of the pedon increased markedly with increasingly mafic composition, more than doubling from rhyolite to andesite, and more than tripling from rhyolite to basalt (Fig. 2b). Amounts of nanocrystalline Fe-(hydr)oxides extractable with acid oxalate (Fe_o) were more variable than Fe_d across the lithosequence and showed no distinct trend relative to parent material (Table 2). The Fe_o/Fe_d ratios were low (<0.18), implying a dominance of crystalline Fe-(hydr)oxides in the pedogenic Fe fraction of all soil horizons. There were no distinct differences in the degree of Fe-(hydr)oxide crystallinity across parent materials. The low oxalate-extractable Si (Si_o) concentrations (<2.0 g kg^{-1}) indicate an absence of allophane and/or imogolite in all pedons. Further, the low active Al_o + 1/2 Fe_o concentrations (<11 g kg^{-1}) indicate the lack of andic soil properties.

3.3. Total elemental analysis

Total Fe (Fe_t) in the <2-mm fraction strongly reflected differences in the initial parent material composition ranging from 4.0% in rhyolite to 11.5% in basalt (Table 3, Fig. 3b).The andesite and dacite pedons had similar Fe_t contents. CaO weight percentages peaked at the surface, ranging from 0.7% to 1.3% in surface horizons, but decreased to <0.6% at depth (Table 3). The increase in CaO at the surface may be the result of nutrient redistribution by deciduous plants (*Quercus* spp.) (Dahlgren et al., 1997b), while the lack of CaO at depth indicates appreciable weathering of calcium containing primary minerals (e.g., plagioclase, augite, amphibole). The Si/Al molar ratios were near 1 across the entire lithosequence (Table 3), suggesting a dominance of 1:1 clay minerals in all soils, except the upper horizon of the rhyolitic soil, where Si/Al ratios were >2. The distinctly elevated Si/Al ratio in the upper horizons of the rhyolite pedon provides additional evidence for a lithologic discontinuity previously suggested by the sharp changes in soil texture, pH and base saturation across the A–B horizon transition.

3.4. P-retention

P-retention varied from 22 to 75% across pedons, and all soil horizons were below the 85% P-retention value required for andic soil properties. Low P-retention values were observed in soils derived from

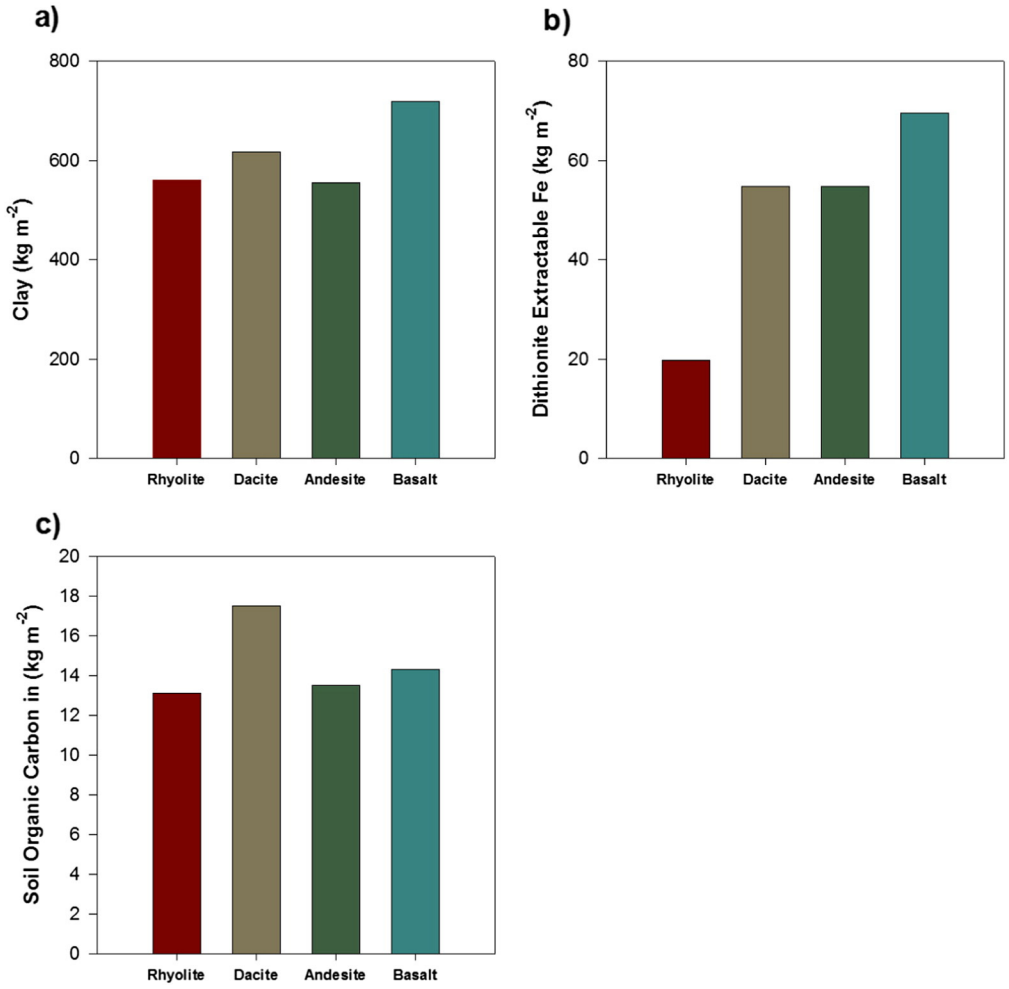

Fig. 2. a) Clay production (kg m^{-2}), b) dithionite-extractable Fe (kg m^{-2}), and c) carbon pools (kg m^{-2}) in the upper 120 cm of the lithosequence pedons.

Table 2
Selective dissolution and P-retention.

Lithology	Horizon	Depth (cm)	Fe_d	Al_d	Fe_o	Al_o	Si_o	$Al_o + 1/2\ Fe_o$	Fe_o/Fe_d ratio	P retention %
			g kg^{-1}							
Rhyolite	Ap1	0–10	14.3	1.9	1.3	1.6	0.3	2.3	0.09	29.1
	Ap2	10–30	15.6	2	1.3	1.6	0.2	2.2	0.08	26.1
	2AB	30–55	17.1	1.8	1.1	1.1	0.3	1.6	0.06	23.2
	2Bt1	55–118	19.6	2.1	0.9	1.3	0.6	1.8	0.05	28.1
	2Bt2	118–155	17.3	1.7	0.5	1.1	0.5	1.4	0.03	22.3
Dacite	A1	0–16	36.7	8.2	3.5	8.8	2.0	10.6	0.10	75.4
	A2	16–30	43.7	7.8	3.7	7.3	1.8	9.1	0.08	63.6
	AB	30–49	45.7	8.0	3.3	5.9	1.6	7.5	0.07	70.4
	Bt1	49–74	47.7	7.5	2.9	4.4	1.5	5.9	0.06	65.8
	Bt2	74–97	35.8	4.0	3.2	3.2	1.1	4.8	0.09	56.8
	Bt3	97–117	33.3	3.5	4.1	3.3	1.2	5.4	0.12	58.2
	BCt	117–150	29.3	2.8	5.2	3.4	1.3	6.0	0.18	57.3
Andesite	A1	0–28	36.7	6.2	2.2	7.3	1.2	8.4	0.06	67.6
	A2	28–79	42.9	5.5	2.1	3.3	0.7	4.4	0.05	55.8
	Bt1	79–99	40.8	4.8	1.5	2.7	0.7	3.4	0.04	54.9
	Bt2	99–152	40.6	4.2	1.5	2.4	0.8	3.2	0.04	53.8
	BCt	152–191	35.5	3.4	2.2	2.6	0.9	3.7	0.06	55.3
Basalt	A1	0–7	46.6	4.8	2.8	7.0	1.4	8.4	0.06	65.1
	A2	7–21	52.1	3.9	3.3	5.6	1.4	7.3	0.06	59.9
	Bt1	21–37	52.9	3.2	3.7	3.4	1.0	5.2	0.07	55.5
	Bt2	37–66	52.7	3.0	3.8	3.2	1.0	5.1	0.07	47.9
	Bt3	66–100	48.1	2.5	3.0	2.1	0.9	3.6	0.06	40.6
	BC	100–120	41.7	2.2	0.3	0.2	1.0	0.3	0.01	36

d = dithionite extractable and o = oxalate extractable.

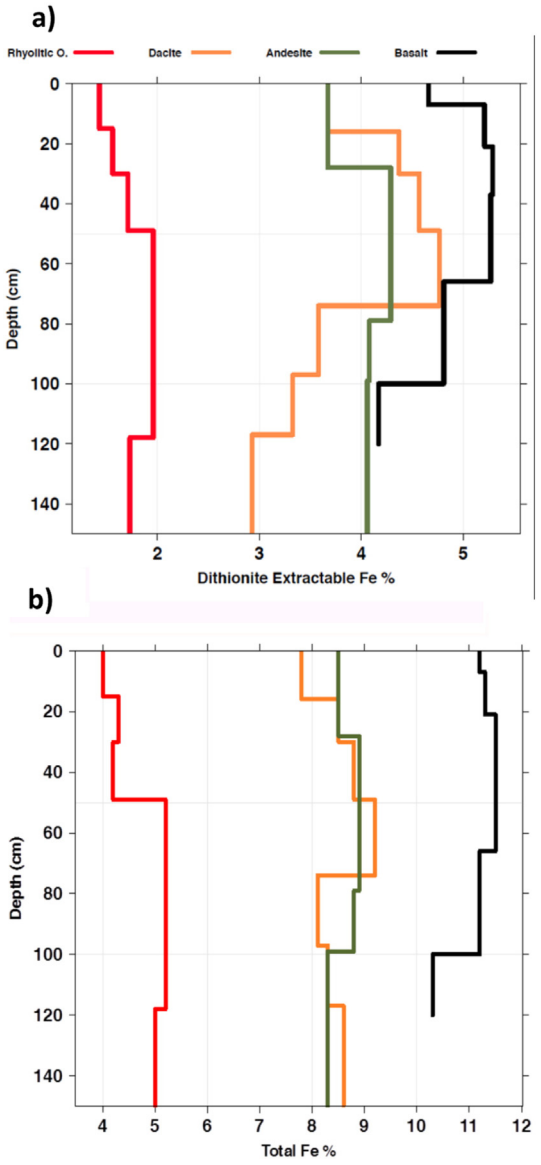

Fig. 3. a) Dithionite-extractable Fe concentrations across parent material compositions as a function of soil depth to 150 cm. b) Total Fe concentrations across parent material compositions as a function of soil depth to 150 cm.

rhyolite (22–29% P-retention) likely due to the low Fe-(hydr)oxide concentrations (<20 g kg^{-1} Fe_d) resulting from the weathering of low Fe content rhyolite. The Fe_d contents were correlated with P-retention ($r = 0.68$, p-value < 0.001), suggesting that the amount of Fe-(hydr)oxides, which is strongly tied to pedon lithology, influences P-retention (Fig. 4a). However, a stronger correlation was observed with the $Al_o + 1/2\ Fe_o$ content ($r = 0.87$, p-value < 0.001) (Fig. 4b) suggesting that nanocrystalline Fe/Al materials exerted a strong influence on P-retention in spite of their low concentration.

3.5. Degree of weathering

The degree of weathering, as expressed by the ratio of pedogenic Fe (Fe_d) to total Fe (Fe_t) was remarkably well constrained across the lithosequence (Fig. 5). The Fe_d/Fe_t ratios averaged 0.43 ± s.e. 0.01, suggesting that despite divergent amounts of Fe_t and Fe_d across the lithosequence, the Fe_d/Fe_t ratios were similar. This relationship is further illustrated by the strong correlation between the amount of Fe available for weathering (Fe_t) and the amount of Fe-(hydr)oxides released by chemical weathering (Fe_d) ($r = 0.95$, p-value < 0.001) (Fig. 5). Thus, soils derived from divergent lithologies with disparate amounts of total Fe, have a similar proportion of their total Fe released by chemical weathering to form pedogenic Fe.

3.6. Clay mineralogy

Identification of clay minerals via XRD revealed a dominance of kaolin mineralogy, with kaolinite and/or halloysite (1.0 nm and 0.7 nm) prevalent, as well as some hydroxy-Al interlayered vermiculite (HIV), and minor gibbsite and vermiculite (Table 4). XRD analysis of the rhyolitic obsidian pedon suggests a clay mineralogy dominated by kaolin minerals (kaolinite and hydrated/dehydrated halloysite), with quartz, cristobalite, minor HIV and gibbsite. Evidence of hydrated (1.0 nm) and dehydrated (0.7 nm expanding to 1.0 nm with formamide) halloysite was found at depth (2Bt1 horizon and deeper). Similarly, the clay fraction from the dacite and andesite pedons indicated dominance of kaolin minerals, in particular halloysite, with the amount of halloysite (0.7 and 1.0 nm) and degree of halloysite hydration increasing with depth. The clay fraction from the basalt pedon was dominantly kaolinite, with vermiculite, minor gibbsite and no distinct halloysite (1.0 nm) phases identified via XRD. Remarkably, soils across the lithosequence converged on kaolin mineralogy, despite the divergent Si concentrations in the various lithologies (Fig. 6).

An increase in halloysite and the degree of halloysite hydration with increasing depth was a common feature for the rhyolite, dacite and andesite pedons, as indicated by a shift from 0.7 nm kaolinite (non-expanding with formamide treatment) to 0.7 nm and 1.0 nm halloysite with increasing depth. Examination of the KCl-saturated (Fig. 7a) and formamide solvated (Fig. 7b) diffractograms in the andesite pedon highlight the increase in halloysite and the degree of halloysite hydration with depth observed for the rhyolite, dacite and andesite pedons.

TEM revealed a dominance of tubular halloysite, with partially subround spherical halloysite, and minor platy kaolinite in the rhyolite, dacite and andesite pedons, exemplified by the andesite Bt1 horizon (Fig. 8a). In contrast, few halloysite tubes were identified throughout the basalt pedon, but rather a dominance of a platy kaolin phase, supporting the lack of appreciable tubular halloysite formation in the basalt pedon (Fig. 8b). SEM with EDX analysis of clay aggregates demonstrated a Si:Al molar ratio of 1.0 with no detectable Fe incorporation (data not shown).

4. Discussion

4.1. Soil genesis

The common weathering environment experienced by the soils of the lithosequence narrowed the trajectory of pedogenesis, resulting in soils from divergent lithologies converging on similar physiochemical properties and dominant kaolin mineralogy, despite a soil residence time estimated to be <10,000 years. As soils undergo pedogenesis, climate exerts greater and greater influence on soil properties, while the influence of parent material is diminished (Jenny, 1941; Jackson, 1959; Chesworth, 1973; Wilson, 1999; Certini and Scalenghe, 2006). Thus, with time and under the influence of climate, the expression of parent material becomes progressively muted. Chesworth (1973) hypothesized that soils from divergent parent materials, such as granite and basalt, should converge to the point where they are relatively indistinguishable, although the amount of time required for parent material effects to be muted was undefined. In light of this, we note that in the mesic-thermic/xeric climate of California, with mild wet winters and dry hot summers, deeply weathered, clay rich, kaolin dominated soils develop in relatively short time periods. Rapid weathering of these glassy, high surface area and high porosity extrusive igneous materials accelerates pedogenesis, independent of the parent material chemical composition.

Table 3
Total elemental analysis (<2-mm fraction).

Lithology	Horizon	Depth (cm)	Major oxides						Zr ppm	Fe_t wt%	Fe_d/Fe_t ratio	Si/Al molar ratio
			SiO_2	Al_2O_3	CaO	MnO_2	Fe_2O_3	TiO_2				
			wt%									
Rhyolite	Ap1	0–10	35.7	13.4	1.3	0.3	5.8	0.8	328	4.0	0.4	2.4
	Ap2	10–30	40.2	15.7	0.8	0.3	6.1	0.9	363	4.3	0.4	2.3
	2AB	30–55	43.3	16.7	0.8	0.2	6.0	0.8	378	4.2	0.4	2.3
	2Bt1	55–118	31.8	22.5	0.6	0.0	7.4	0.7	472	5.2	0.4	1.3
	2Bt2	118–155	31.1	21.7	0.6	0.0	7.1	0.7	447	5.0	0.3	1.3
Dacite	A1	0–16	24.1	16.6	1.2	0.3	11.2	1.1	199	7.8	0.5	1.3
	A2	16–30	26.4	17.7	0.7	0.3	12.2	1.2	228	8.5	0.5	1.3
	AB	30–49	25.5	18.1	0.6	0.3	12.5	1.1	217	8.8	0.5	1.2
	Bt1	49–74	27.0	20.0	0.5	0.2	13.2	0.9	232	9.2	0.5	1.2
	Bt2	74–97	27.8	19.7	0.5	0.1	11.6	0.9	196	8.1	0.4	1.2
	Bt3	97–117	27.1	18.8	0.5	0.1	11.9	0.9	178	8.3	0.4	1.3
	BCt	117–150	26.2	18.6	0.5	0.2	12.3	1.0	160	8.6	0.3	1.2
Andesite	A1	0–28	27.6	17.6	0.7	0.3	12.1	1.0	239	8.5	0.4	1.4
	A2	28–79	27.0	17.6	0.5	0.1	12.7	1.0	243	8.9	0.5	1.4
	Bt1	79–99	27.6	19.1	0.4	0.1	12.6	0.9	240	8.8	0.5	1.3
	Bt2	99–152	26.6	19.3	0.5	0.1	11.9	0.9	227	8.3	0.5	1.2
	BCt	152–191	25.2	18.7	0.4	0.1	11.9	0.9	218	8.4	0.4	1.2
Basalt	A1	0–7	23.6	16.3	1.2	0.4	16.0	1.3	250	11.2	0.4	1.3
	A2	7–21	23.7	16.1	0.8	0.4	16.1	1.3	242	11.3	0.5	1.3
	Bt1	21–37	24.0	16.0	0.7	0.4	16.4	1.3	254	11.5	0.5	1.3
	Bt2	37–66	25.1	16.9	0.6	0.4	16.4	1.3	260	11.5	0.5	1.3
	Bt3	66–100	26.5	17.7	0.6	0.2	16.0	1.2	228	11.2	0.4	1.3
	BC	100–120	25.9	16.1	0.6	0.1	14.7	1.1	212	10.3	0.4	1.4

In contrast, Fe is conserved during pedogenesis, and differences in the initial Fe content of parent materials are expressed as differences in Fe-(hydr)oxide content of soils. The effect of weathering is constant across lithologies such that the ratio of Fe weathered (Fe_d) to total Fe (Fe_t) is consistent, regardless of initial parent material Fe content. In this respect, both the overwhelming effects of climate, and the enduring influence of parent material, are exemplified in the lithosequence. Climate and time have subdued the parent material effect on clay mineralogy, and constricted the trajectory of pedogenesis, while the influence of parent material endures as differences in Fe-(hydr)oxide content.

4.2. Soil physiochemical properties

Soils from the lithosequence displayed remarkable similarities for several physiochemical parameters. The CEC, pH, base saturation and soil texture generally converged in spite of strongly contrasting parent materials to a slightly acidic pH (H_2O), evidence of clay illuviation and argillic horizon formation, high base saturation and low CEC. The high base saturation and slightly acidic soil conditions, in spite of the advanced stage of weathering and soil development, may speculatively result from the input of bases due to occasional volcanic ash inputs. Soil carbon storage was similar across the lithosequence, with the exception of the dacite pedon, which was recently converted from wildland to winegrape production (Fig. 2c). These data suggest that parent material composition is not a driving factor regulating carbon sequestration in this lithosequence. This is in agreement with the findings of Heckman et al. (2014), who found no significant differences in soil organic carbon or occluded soil organic matter attributable to variations in lithology, concluding that climate, fire frequency and preferential occlusion of charcoal are more substantial factors in carbon dynamics than initial parent material composition.

Convergence of soil physiochemical parameters suggests that the common weathering environment experienced by the diverse lithologies functioned to narrow the trajectory of pedogenesis. This is in contrast with the findings of previous lithosequences. For example, Parsons and Herriman (1975) found differences in CEC and soil texture between granite and schist versus volcanic tuff, breccia and pyroclastics, in soils above the winter snowline. Those pedons were found in a much cooler climate, suggesting that the rate of pedogenesis was comparatively slowed. Similarly, Heckman and Rasmussen (2011) investigated a lithosequence that contained two volcanic parent materials, and concluded that diverse lithologies resulted in soils with substantial differences in soil morphological and physiochemical properties. However, soils from their study were less weathered than the soils in this study, showing more strongly the influence of parent material. For example, the basalt soil of Heckman and Rasmussen (2011) had a maximum Fe_d content of 27 g kg^{-1}, compared to 52.9 g kg^{-1} in this study. Less strongly weathered soils maintain characteristics of their parent material, and exhibit less of the unifying effect of a common climate on soil mineralogy and physicochemical properties (Jenny, 1941; Jackson, 1959; Chesworth, 1973; Wilson, 1999; Certini and Scalenghe, 2006).

Chesworth (1973), in an assessment of the effect of parent material on soil formation, concluded that soils become physicochemically and mineralogically similar with time and common weathering. This is in agreement with several climosequences that have confirmed climate as a strong driver of pH, clay percent, CEC and BS, within a specific lithology in the mesic/xeric climate of California (Dahlgren et al., 1997a; Rasmussen et al., 2007, 2010). The common, strong weathering environment endured by the lithosequence functions to reduce the influence of parent material on soil physicochemical properties through time, resulting in the convergence of soil BS, CEC, pH, clay illuviation and clay production observed. This convergence suggests that as soils undergo pedogenesis, climate eventually dampens the influence of lithology on soil physicochemical and morphological properties, in all but the most extreme cases of lithologic differences.

4.3. Fe-(hydr)oxides and relative degree of weathering

Lithology exerted a substantial influence on total Fe (Fe_t) and pedogenic Fe (Fe_d) contents. This result is in agreement with those from climosequences on basalt (Rasmussen et al., 2010) and andesite (Rasmussen et al., 2007), where a similar amount of Fe_d and Fe_t was found in a similar climate regime (mesic/xeric). For example, Rasmussen et al. (2010) found between 46 and 59 g kg^{-1} Fe_d, and 15–17% Fe_2O_3 Fe_t in basalt soils, in good agreement with the 41–53 g kg^{-1} Fe_d and 15–16% Fe_2O_3 Fe_t found in the basalt pedon in this study. In contrast, lower Fe_d values were found on granitic lithologies

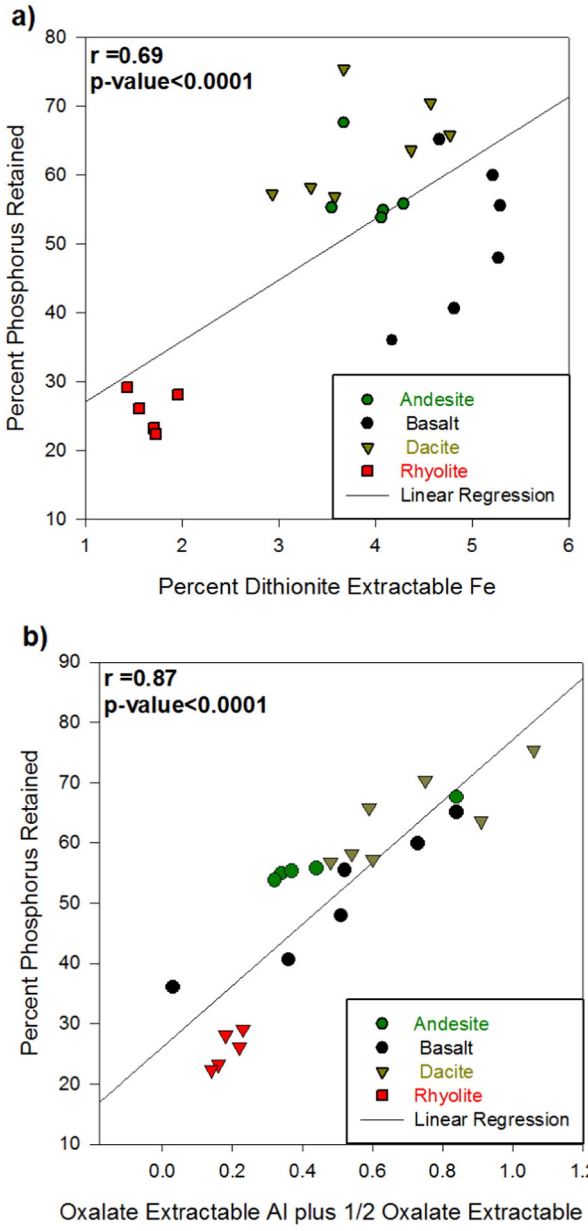

Fig. 4. a) Relationship between pedogenic Fe and phosphorus retention. b) Relationship between nanocrystalline Fe and Al materials and phosphorus retention.

from a similar climate (Dahlgren et al., 1997a) while greater crystalline Fe-oxides were observed in a similarly weathered rhyolitic tephra in New Zealand (Bakker et al., 1996), as compared to the rhyolite pedon in this study. Differences in grain size between parent materials of similar elemental composition may account for the differences in Fe_d production in rhyolitic tephra (extrusive) and granite (intrusive) noted in previous studies, and the Fe_d production in the rhyolitic obsidian (extrusive) in this study. That both Fe_t and Fe_d contents increase with the increasingly mafic composition of lithology asserts that Fe content is both divergent across the lithosequence and conserved during pedogenesis.

While amounts of Fe_t and Fe_d diverged, the relative degree of weathering was well constrained across the lithosequence as assessed by the Fe_d:Fe_t ratio. The Fe_d:Fe_t ratio fell in a relatively narrow range between 0.35 and 0.52 irrespective of differences in parent material Fe composition. Similar values were found in the aforementioned climosequences on basalt and andesite (Rasmussen et al., 2007, 2010). The Fe_d and Fe_t concentrations

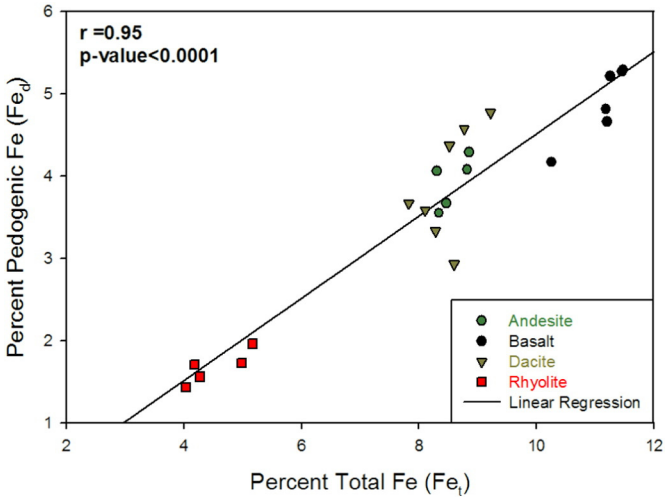

Fig. 5. Relationship between total Fe and pedogenic Fe across the lithosequence.

were strikingly well correlated ($r = 0.95$); as the total amount of Fe increased, the amount of Fe chemically weathered to Fe_d increased in a relatively constant proportion. These findings are consistent with those of Fritz (1988) who found that Fe behaved similarly in weathering rinds of both gabbro and granite. The Fe^{2+}/Fe^{3+} ratio, used as an indicator for the weathering of primary mineral Fe (Fe^{2+}) to secondary Fe-(hydr)oxides (Fe^{3+}), was similar in both weathering rinds despite the contrasting lithologies and total Fe contents. Similar to our study, Fritz (1988) found that, although gabbro produced twice as much secondary Fe-(hydr)oxides, the Fe^{2+}/Fe^{3+} ratio was similar in the weathering rinds of both granite and gabbro.

Soils of the lithosequence were consistently dominated by crystalline Fe-(hydr)oxides as opposed to nanocrystalline forms (as defined by Fe_o), suggesting that the common pedogenic environment likely controls the form of Fe-(hydr)oxides present. The Fe_o/Fe_d ratios were <0.18 across all horizons and lithologies. Low Fe_o/Fe_d ratios reflect both the advanced stage of pedogenesis and the preference for crystalline pedogenic Fe in xeric soils experiencing pronounced seasonal desiccation (Schwertmann, 1985; Takahashi et al., 1993; Dahlgren et al., 1997a, 1997b; Rasmussen et al., 2007, 2010). The dominance of crystalline Fe-(hydr)oxides has been previously reported in granite, andesite and basalt experiencing a similar pedogenic environment, and a rhyolitic tephra with a similar degree of pedogenesis (Takahashi et al., 1993; Bakker et al., 1996; Dahlgren et al., 1997a; Rasmussen et al., 2007, 2010). Seasonal desiccation in warm, xeric environments, along with low organic matter and silica activities, favors the formation of crystalline Fe-oxide minerals, rather than hydrated or nanocrystalline sesquioxides (Schwertmann, 1985; Takahashi et al., 1993). We suggest that divergence in Fe_t and Fe_d concentrations reflects differences in the initial elemental composition of the parent material, while similarities in the degree of weathering and the dominance of crystalline Fe-(hydr)oxides suggest processes attributable to the common climate experienced by the lithosequence.

4.4. Phosphorus retention

The influence of lithology on P dynamics was suggested by Walker and Syers (1976), and more recently investigated by Porder and Ramachandran (2013). Dieter et al. (2010) suggested that the initial chemical composition of the parent material may influence P dynamics, through its influence on soil Al and Fe concentrations. The influence of lithology on P-retention is evident in the rhyolite pedon, which had markedly lower Fe_t and Fe_d and subsequently the lowest P-retention, as compared to the more mafic soils. Fe_d showed a weak correlation

Table 4
Clay mineralogy of Clear Lake Volcanic Field lithosequence as identified by X-ray diffraction.

Horizon	Rhyolite	Horizon	Dacite	Horizon	Andesite	Horizon	Basalt
Ap1	KK (M) †, HV (m)‡, VR (m)	A1	KK (M), KH (m), HV (m), GI (m)	A1	KK (M), KH (m), HV (m), GI (m)	A1	KK (M), HV (m), CL (m), GI (m)
Ap2	KK (M), HV (m)	A2	KH (M), KK (M), HV (m), GI (m)	A2	KH (M), KK (M), HV (m), GI (m)	A2	KK (M), HV (m), VR (m), GI (m)
2AB	KK (M), HV (m)	AB	KH (M), KK (m), HV (m), GI (m)	Bt1	KH (M), KK (m), HV (m), GI (m)	Bt1	KK (M), HV (m), VR (m), GI (m)
2Bt1	KH (M), KK (M), HV (m)	Bt1	KH (M), KK (M), HV (m), GI (m)	Bt2	KH (M)	Bt2	KK (M), HV (m), VR (m), GI (m)
2Bt2	KH (M), KK (M), HV (m)	Bt2	KH (M), KK (m), GI (m), HV (m)	BCt	KH (M)	Bt3	KK (M), HV (m), VR (m)
		Bt3	KH (M), GI (m), HV (m)				
		BCt	KH (M)				

Mineralogical codes: KK = kaolinite, HV = hydroxy interlayered vermiculite, VR = vermiculite, KH = halloysite, GI = gibbsite, and CL = chlorite. †M = Major, ‡m = Minor.

with phosphorus retention, suggesting that initial parent material Fe content, and hence Fe_d, exerts some control on P dynamics. However, less prominent nanocrystalline Fe/Al-(hydr)oxides, represented by $Al_o + 1/2\ Fe_o$, were more strongly correlated with P-retention, suggesting that the crystallinity of the Fe/Al-(hydr)oxides contributes significantly to P retention dynamics. Thus, although the amount of nanocrystalline Fe/Al-(hydr)oxides was small, they exert a substantial influence on P-retention dynamics, and represent an important portion of the P-sorption capacity. This is consistent with the findings of Johnson et al. (1986) who concluded that nanocrystalline Fe/Al-(hydr)oxides exert a greater influence on anion sorption than crystalline Fe/Al-(hydr)oxides. High surface area, significant variable charge and multiple anion sorption sites, attributable to nanocrystalline Fe/Al-(hydr)oxides, contribute to the dominant influence of nanocrystalline constituents on P-retention (Parfitt, 1979, 1989). Thus, both the crystallinity of Fe-(hydr)oxides, which is largely driven by soil microclimate and precipitation and desiccation cycles, and the amount of Fe-(hydr)oxides, itself dependent on lithology, may influence P-dynamics. However, more research is required to confirm the influence of climate and lithology on P dynamics. The variability in P-retention, which ranged from 23 to 75%, suggests that P dynamics may be considerably variable to warrant differential soil P management strategies.

4.5. Phyllosilicate mineralogy

In spite of their strongly divergent lithologies, the clay mineralogical composition converged on kaolin minerals (halloysite and kaolinite). Desilication, kaolinitization and the degree of clay mineral crystallization, processes and factors attributable to a common pedogenic environment, were the primary mechanisms controlling clay mineral transformations and neogenesis across the lithosequence. Si:Al ratios were <1.4 (<2-mm fraction), except in the upper horizons of the rhyolitic soil, substantiating desilication as a major process. In contrast to Rasmussen et al. (2010), smectite was not observed in the basalt pedon of this study. Rasmussen et al. (2010) attributed the formation of smectite occurring preferentially at the soil-bedrock interface to the interaction of localized poor drainage conditions, resulting in the accumulation of solutes at the soil-bedrock interface and the relatively slow drying of the lower soil profile. In contrast, Ziegler et al. (2003) concluded that seasonal wet-dry cycles and arid conditions favor the formation of kaolin minerals relative to smectite in Hawaiian basalts, with nanocrystalline minerals serving as a metastable precursor to halloysite. Delvaux et al. (1990) identified halloysite-smectite intergrades in basic igneous materials in tropical climates, and suggested a progression from allophanic metastable precursors to smectite and smectite-halloysite intergrades, to dominantly kaolinite and smectite-halloysite intergrades with progressive weathering. The progression of smectite to smectite-kaolinite to dominantly kaolinite was demonstrated in a basalt toposequence in a Mediterranean climate, with kaolinite dominant in well drained soils of the shoulder positions (Vingiani et al., 2004).

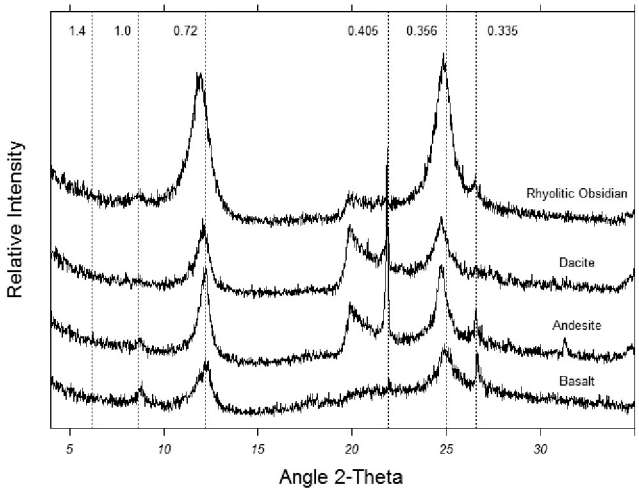

Fig. 6. X-ray diffractograms for KCl-350 °C heated clay fraction of Bt2 horizons from all lithologies. Diffractograms show a convergence on kaolin mineralogy across the lithosequence, as shown by the dominant ~0.7 nm peak. Drop lines are mineral d-spacings in nm.

The basalt pedon in this study, itself well-drained and formed at a shoulder position, had a clay fraction that was dominantly kaolinite, lacking both smectite, and appreciable tubular halloysite (0.7 and 1.0 nm), as inferred from XRD and TEM analyses. Potentially, the kaolinite in the basalt pedon may be formed via the progression from smectite to smectite-kaolin to dominantly kaolinite through dissolution and progressive desilication of smectite-kaolin intergrades, coupled with dehydration and collapse of any proto-halloysite formed in intermediate stages (Delvaux et al., 1990; Ryan and Huertas, 2009; Vingiani et al., 2004). However, no evidence of smectite or smectite-intergrades was observed in this study. Potentially, the high Fe content in basalt could result in substitution of Fe for Al in octahedra, disfavoring tubular halloysite formation in favor of platy halloysite and kaolinite (Joussein et al., 2005). However, the SEM with EDX analysis did not detect Fe in clay aggregates from the basalt clay fraction. Alternatively, the lack of both smectite and halloysite is consistent with low Si activities in soils formed in volcanic ejecta (Shoji et al., 1993). The basalt parent material has the lowest potential aqueous Si activities given the low Si content of basalt among the various lithologies, disfavoring smectite and halloysite formation. Furthermore, the shoulder landscape position has good downslope drainage favoring removal of Si and other bases, which may hinder smectite and halloysite formation, consistent with the observation of kaolinite dominance in the shoulder position on basalt parent material (Vingiani et al., 2004). Without the localized poor drainage conditions at the soil-bedrock interface, there remains no mechanism to impede drainage and allow accumulation of Si and other bases. Therefore, we speculate that a Si activity threshold was passed in the basalt profile that favors direct formation of a platy kaolinite at the expense of smectite and tubular halloysite.

An increase in halloysite and the degree of halloysite hydration was shared by all but the most mafic end-member of the lithosequence as is

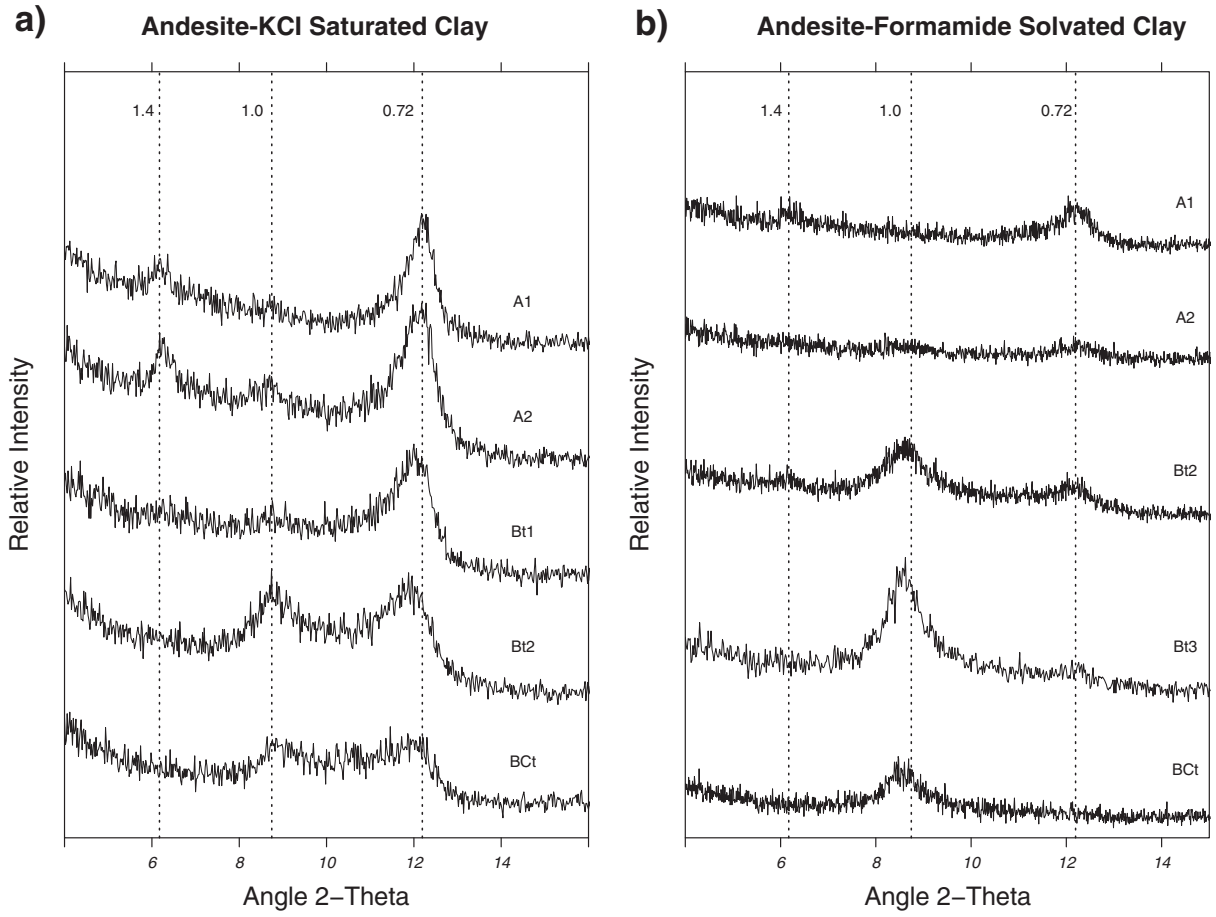

Fig. 7. a) X-ray diffractograms for KCl saturated clay fraction of andesite soil, from surface horizon to depth. Diffractograms show a shift in the amount of halloysite and the degree halloysite hydration with increasing depth as indicated by a shift from 0.7 nm to 1.0 nm, and shouldering from 0.7 nm to 1.0 nm with increasing depth. b) X-ray diffractograms of KCl saturated and formamide solvated clay fraction of andesite soils show a shift from 0.7 nm kaolinite to 1.0 nm halloysite with increasing depth. Drop lines are mineral d-spacings in nm.

commonly observed in soils from xeric climates in California (Southard and Southard, 1987; Takahashi et al., 1993; Rasmussen et al., 2007, 2010). Deeper soil horizons tend to remain relatively moist throughout the year maintaining the hydration of halloysite, while the upper soil profile is strongly desiccated during the summer dry season. This desiccation favors the dehydration of tubular halloysite to a tubular kaolin mineral that does not expand with formamide solvation in the upper soil horizons (Takahashi et al., 2001). We conclude that tubular 1:1 kaolin minerals persist in different degrees of hydration and expandability from surface to depth in the soils formed on rhyolite, dacite and andesite.

The subsoil horizons of the rhyolitic soil were strongly weathered with peak clay concentrations of 782 g kg^{-1}. The high clay content is consistent with similarly weathered rhyolitic soils in New Zealand (Bakker et al., 1996). Interestingly, obsidian clasts in the lower soil horizons appeared relatively unweathered in a matrix of highly weathered soil. We speculate that this results from the differential weathering of rhyolitic tephra/pumice interspersed with the rhyolitic obsidian during deposition. The porous tephra/pumice component will weather much more rapidly and completely compared to the relatively non-porous obsidian clasts. This rapid weathering of the tephra/pumice component within the obsidian flows manifests itself as fresh-looking obsidian clasts in the highly weathered matrix containing nearly 800 g kg^{-1} clay. This potential mechanism suggests that differences in depositional environment, grain size and surface area/porosity may strongly influence differences in chemical weathering and soil texture within parent materials of similar chemical composition.

The lack of nanocrystalline (allophane) and paracrystalline (imogolite) aluminosilicates across the lithosequence is consistent with other soils derived from volcanic-ejecta in mesic/xeric environments of California (Takahashi et al., 1993; Dahlgren et al., 1997a; Rasmussen et al., 2007, 2010). In contrast, weathering of tephra deposits in mesic/udic climatic regimes, such as in northern Japan, yields a prevalence of nanocrystalline and paracrystalline materials (e.g., allophane, imogolite, ferrihydrite) with few crystalline minerals at a similar early stage of weathering (<10,000 yr) (Shoji et al., 1993). This suggests that the distinct wet and dry periods associated with the xeric soil moisture regime have a profound influence on the weathering products of extrusive igneous parent materials, regardless of initial elemental composition. Crystallinity of clay minerals is favored in xeric climates, where Ostwald ripening (dissolution and reprecipitation) and dehydration are energetically and kinetically favored by prolonged periods of high temperature and desiccation during the summer dry period (Takahashi et al., 1993; Ziegler et al., 2003). Ziegler et al. (2003) noted that harsh drying quickly promotes the formation of crystallized kaolin minerals from allophanic precursors in basalt soils from Hawaii. In rhyolitic soils in New Zealand, drier conditions also favored halloysite formation at the expense of nanocrystalline materials (Parfitt et al., 1983). Similar results were noted in trachydacitic soils in Italy, where embryonic halloysite formed but not appreciable allophane (Certini et al., 2006). Thus, the initial chemical composition of lithology appears to exert little influence on the degree of clay mineral crystallinity or the persistence of nanocrystalline minerals. Instead soil microclimate and precipitation-desiccation cycles (xeric soil moisture regime) drive the degree of

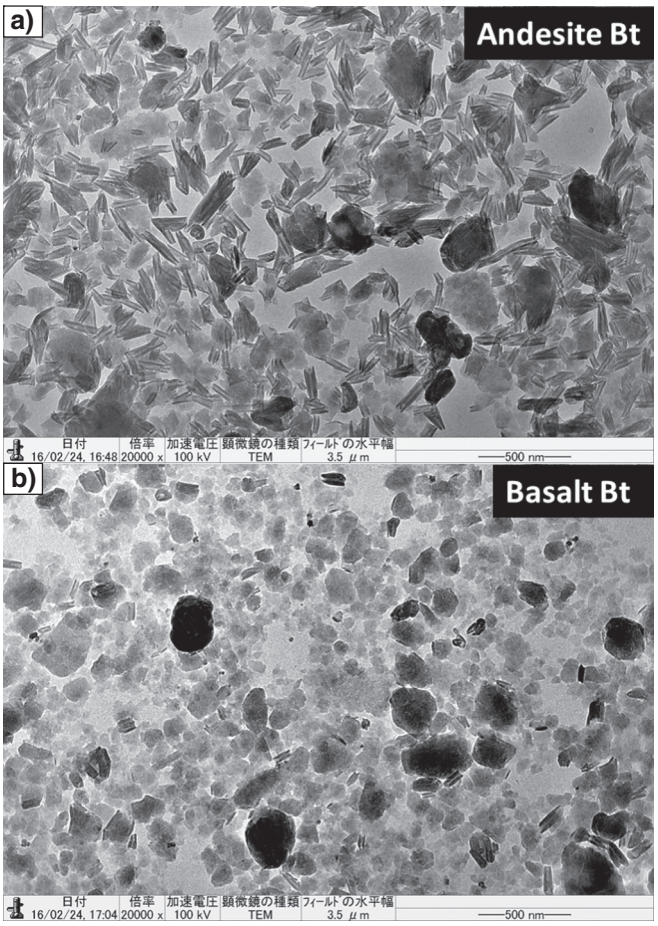

Fig. 8. Transmission electron micrographs of clay fraction from a) andesite Bt horizon revealing significant halloysite tubules and b) basalt Bt horizon revealing trace halloysite tubules and dominance of kaolinite plates and aggregates.

crystallinity and form of clay minerals at the expense of nanocrystalline weathering products.

5. Conclusion

Lithology is a master variable of soil formation, and yet very few highly constrained lithosequences have been investigated. Here, a well-constrained soil lithosequence on extrusive igneous materials consisting of rhyolite, dacite, andesite and basalt was utilized to explore the influence of lithology on soil genesis, soil physiochemical properties, Fe-(hydr)oxide generation, and clay mineral formation. Soils from diverse initial chemical compositions experienced a common pedogenic environment, manifest in mild wet winters which favor desilication/leaching and warm dry summers that desiccate the soil pedon favoring crystallization and kaolin dehydration. The effects of climate and time function to restrict the influence of lithology on clay mineral neogenesis, with soils from divergent lithologies converging on kaolin mineralogy, all likely within the Holocene. While the influence of climate subdued the parent material effect on silicate clays, the imprint of parent material Fe content is maintained during pedogenesis, evident in differences in total and pedogenic Fe content and P-retention. In both Fe-(hydr)oxides and phyllosilicate clays, crystallization is favored at the expense of hydrated Fe-(hydr)oxides and nanocrystalline aluminosilicates, regardless of initial parent material chemical composition; the result of seasonal desiccation during the summer dry season. Halloysite formation and varying degrees of halloysite hydration were common features of the rhyolitic, dacitic and andesitic lithologies. A common weathering environment may eventually result in soils from divergent lithologies being morphologically and clay mineralogically indistinguishable. We conclude that the transformative effect of time and a common climate functioned to narrow pedogenesis, resulting in the strong convergence of soil physicochemical properties and kaolin clay minerals across the lithosequence. However, the enduring imprint of lithology is manifest in differences in total Fe and pedogenic Fe, with these differences maintained through pedogenesis.

References

Anderson, J., Bailey, O., Rai, D., 1975. Effects of parent material on genesis of Borolls and Boralfs in south-central New Mexico mountains. Soil Sci. Soc. Am. J. 39 (5), 901–904.

Bakker, L., Lowe, D.J., Jongmans, A., 1996. A micromorphological study of pedogenic processes in an evolutionary soil sequence formed on Late Quaternary rhyolitic tephra deposits, North Island, New Zealand. Quat. Int. 34, 249–261.

Balco, G., Finnegan, N., Gendaszek, A., Stone, J.O., Thompson, N., 2013. Erosional response to northward-propagating crustal thickening in the coastal ranges of the US Pacific Northwest. Am. J. Sci. 313 (8), 790–806.

Blakemore, L., Searle, P.L., Daly, B.K., Bureau, S., 1981. Soil bureau laboratory methods: methods for chemical analysis of soils. A. Department of Scientific and Industrial Research. New Zealand Soil Bureau Scientific Report 80 (Lower Hutt, New Zealand).

Certini, G., Scalenghe, R., 2006. Soils: Basic Concepts and Future Challenges. Cambridge University Press, Cambridge.

Certini, G., Wilson, M.J., Hillier, S.J., Fraser, A.R., Delbos, E., 2006. Mineral weathering in trachydacitic-derived soils and saprolites involving formation of embryonic halloysite and gibbsite at Mt. Amiata, Central Italy. Geoderma 133 (3), 173–190.

Chadwick, O.A., Kelly, E.F., Merritts, D.M., Amundson, R.G., 1994. Carbon dioxide consumption during soil development. Biogeochemistry 24 (3), 115–127.

Chesworth, W., 1973. The parent rock effect in the genesis of soil. Geoderma 10 (3), 215–225.

Churchman, G.J., Theng, B.K.G., Claridge, G.G.C., Theng, B.K.G., 1984. Intercalation method using formamide for differentiating halloysite from kaolinite. Clay Clay Miner. 32 (4), 241–248.

Dahlgren, R., Boettinger, J., Huntington, G., Amundson, R., 1997a. Soil development along an elevational transect in the western Sierra Nevada, California. Geoderma 78 (3), 207–236.

Dahlgren, R.A., Singer, M.J., Huang, X., 1997b. Oak tree and grazing impacts on soil properties and nutrients in a California oak woodland. Biogeochemistry 39 (1), 45–64.

Delvaux, B., Herbillon, A.J., Vielvoye, L., Mestdagh, M.M., 1990. Surface properties and clay mineralogy of hydrated halloysitic soil clays. ii: Evidence for the presence of halloysite/smectite (h/sm) mixed-layer. Clay Miner. 25, 141–160.

Dieter, D., Elsenbeer, H., Turner, B.L., 2010. Phosphorus fractionation in lowland tropical rainforest soils in central Panama. Catena 82 (2), 118–125.

Donnelly-Nolan, J.M., Hearn Jr., B.C., Curtis, G.H., Drake, R.E., 1981. Geochronology and evolution of the Clear Lake Volcanics. US Geol. Surv. Prof. Pap. 1141, 47–60.

Fritz, S.J., 1988. A comparative study of gabbro and granite weathering. Chem. Geol. 68 (3), 275–290.

Hahm, W.J., Riebe, C.S., Lukens, C.E., Araki, S., 2014. Bedrock composition regulates mountain ecosystems and landscape evolution. Proc. Natl. Acad. Sci. 111 (9), 3338–3343.

Hearn, B.C., Donnelly-Nolan, J.M., Goff, F., 1975. Geology and geochronology of the Clear Lake volcanics, California. US Geological Survey. Open-File Report 75-296 (18 pp.).

Hearn Jr., B.C., Donnelly, J.M., Goff, F.E., 1995. Geologic map and structure sections of the Clear Lake volcanics, northern California. US Geological Survey Miscellaneous Investigation Series Map I-2362.

Heckman, K., Rasmussen, C., 2011. Lithologic controls on regolith weathering and mass flux in forested ecosystems of the southwestern USA. Geoderma 164 (3), 99–111.

Heckman, K., Throckmorton, H., Clingensmith, C., Vila, F.J.G., Horwath, W.R., Knicker, H., Rasmussen, C., 2014. Factors affecting the molecular structure and mean residence time of occluded organics in a lithosequence of soils under ponderosa pine. Soil Biol. Biochem. 77, 1–11.

Holmgren, G.G., 1967. A rapid citrate-dithionite extractable iron procedure. Soil Sci. Soc. Am. Proc. 31 (2), 210–211.

Hoyum, R., Hajek, B., 1979. A lithosequence in coastal plain sediments in Alabama. Soil Sci. Soc. Am. J. 43 (1), 151–156.

Hutton, C.E., 1951. Studies of the chemical and physical characteristics of a chrono-lithosequence of loess-derived prairie soils of southwestern Iowa. Soil Sci. Soc. Am. J. 15, 318–324 (l).

Jackson, M., 1959. Frequency distribution of clay minerals in major great soil groups as related to the factors of soil formation. Clay Clay Miner. 6, 133–143.

Jenny, H., 1941. Factors of Soil Formation. McGraw-Hill Book Company New York, NY.

Jenny, H., 1994. Factors of Soil Formation: A System of Quantitative Pedology. Courier Corporation.

Johnson, D.W., Cole, D.W., Van Miegroet, H., Horng, F.W., 1986. Factors affecting anion movement and retention in four forest soils. Soil Sci. Soc. Am. J. 50 (3), 776–783.

Joussein, E., Petit, S., Churchman, J., Theng, B., Righi, D., Delvaux, B., 2005. Halloysite clay minerals - a review. Clay Miner. 40 (4), 383–426.

Lenton, T.M., Crouch, M., Johnson, M., Pires, N., Dolan, L., 2012. First plants cooled the Ordovician. Nat. Geosci. 5 (2), 86–89.

Levine, S.J., Hendricks, D.M., Schreiber, J.F., 1989. Effect of bedrock porosity on soils formed from dolomitic limestone residuum and eolian deposition. Soil Sci. Soc. Am. J. 53 (3), 856–862.

Mareschal, L., Turpault, M.P., Ranger, J., 2015. Effect of granite crystal grain size on soil properties and pedogenic processes along a lithosequence. Geoderma 249, 12–20.

Morford, S.L., Houlton, B.Z., Dahlgren, R.A., 2011. Increased forest ecosystem carbon and nitrogen storage from nitrogen rich bedrock. Nature 477, 78–81.
Parfitt, R., 1979. Anion adsorption by soils and soil materials. Adv. Agron. 30, 1–50.
Parfitt, R., 1989. Phosphate reactions with natural allophane, ferrihydrite and goethite. J. Soil Sci. 40 (2), 359–369.
Parfitt, R., Russell, M., Orbell, G., 1983. Weathering sequence of soils from volcanic ash involving allophane and halloysite, New Zealand. Geoderma 29 (1), 41–57.
Parsons, R.B., Herriman, R.C., 1975. A lithosequence in the mountains of southwestern Oregon. Soil Sci. Soc. Am. J. 39 (5), 943–948.
Porder, S., Ramachandran, S., 2013. The phosphorus concentration of common rocks - a potential driver of ecosystem P status. Plant Soil 367 (1–2), 41–55.
Rasmussen, C., Matsuyama, N., Dahlgren, R.A., Southard, R.J., Brauer, N., 2007. Soil genesis and mineral transformation across an environmental gradient on andesitic lahar. Soil Sci. Soc. Am. J. 71 (1), 225–237.
Rasmussen, C., Dahlgren, R.A., Southard, R.J., 2010. Basalt weathering and pedogenesis across an environmental gradient in the southern Cascade Range, California, USA. Geoderma 154 (3), 473–485.
Ryan, P., Huertas, F.J., 2009. The temporal evolution of pedogenic Fe-smectite to Fe-kaolin via interstratified kaolin-smectite in a moist tropical soil chronosequence. Geoderma 151 (1), 1–15.
Schaetzl, R.J., 1991. A lithosequence of soils in extremely gravelly, dolomitic parent materials, Bois Blanc Island, Lake Huron. Geoderma 48 (3), 305–320.
Schwertmann, U., 1985. The effect of pedogenic environments on iron oxide minerals. Adv. Soil Sci.Springer, pp. 171–200
Shoji, S., Nanzyo, M., Dahlgren, R., 1993. Volcanic Ash Soils: Genesis, Properties and Utilization. Elsevier.
Soil Survey Staff, 2014a. Keys to Soil Taxonomy. 12th ed. U.S. Department of Agriculture, Natural Resources Conservation Service.
Soil Survey Staff, 2014b. Kellogg soil survey laboratory methods manual. Soil Survey Investigations Report No. 42, Version 5.0. U.S. Department of Agriculture, Natural Resources Conservation Service.
Southard, R., Southard, S., 1987. Sand-sized kaolinized feldspar pseudomorphs in a California Humult. Soil Sci. Soc. Am. J. 51 (6), 1666–1672.
Takahashi, T., Dahlgren, R., van Susteren, P., 1993. Clay mineralogy and chemistry of soils formed in volcanic materials in the xeric moisture regime of northern California. Geoderma 59 (1), 131–150.
Takahashi, T., Dahlgren, R., Theng, B., Whitton, J., Soma, M., 2001. Potassium-selective, halloysite-rich soils formed in volcanic materials from Northern California. Soil Sci. Soc. Am. J. 65 (2), 516–526.
Vingiani, S., Righi, D., Petit, S., Terribile, F., 2004. Mixed-layer kaolinite-smectite minerals in a red-black soil sequence from basalt in Sardinia (Italy). Clay Clay Miner. 52 (4), 473–483.
Walker, T., Syers, J.K., 1976. The fate of phosphorus during pedogenesis. Geoderma 15 (1), 1–19.
Willen, D.W., 1965. Surface soil textural and potential erodibility characteristics of some southern Sierra Nevada forest sites. Soil Sci. Soc. Am. Proc. 29 (2), 213–218.
Wilson, M.J., 1999. The origin and formation of clay minerals in soils: past, present and future perspectives. Clay Miner. 34 (1), 7–24.
Yassoglou, N., Nobeli, C., Vrahamis, S., 1969. A study of some biosequences and lithosequences in the zone of Brown Forest soils in northern Greece: morphological, physical, and chemical properties. Soil Sci. Soc. Am. J. 33 (2), 291–296.
Yousefifard, M., Ayoubi, S., Poch, R.M., Jalalian, A., Khademi, H., Khormali, F., 2015. Clay transformation and pedogenic calcite formation on a lithosequence of igneous rocks in northwestern Iran. Catena 133, 186–197.
Ziegler, K., Hsieh, J.C., Chadwick, O.A., Kelly, E.F., Hendricks, D.M., Savin, S.M., 2003. Halloysite as a kinetically controlled end product of arid-zone basalt weathering. Chem. Geol. 202 (3), 461–478.